Geophysical Journal International

Geophys. J. Int. (2023) **234,** 2066–2074
Advance Access publication 2023 May 4
GJI Geodynamics and Tectonics

https://doi.org/10.1093/gji/ggad189

Remaining non-isostatic effects in isostatic-gravimetric Moho determination—is it needed?

M. Abrehdary [1] and L. E. Sjöberg [1,2]

[1] *Department of Earth Sciences, Division of Geophysics, Uppsala University (UU), SE-75236 Uppsala, Sweden. E-mail: majid.abrehdary@geo.uu.se*
[2] *Division of Geodesy and Satellite Positioning, Royal Institute of Technology (KTH), SE-10044 Stockholm, Sweden*

Accepted 2023 April 20. Received 2023 March 17; in original form 2022 December 31

SUMMARY

For long time the study of the Moho discontinuity (or Moho) has been a crucial topic in inferring the dynamics of the Earth's interior, and with profitable result it is mapped by seismic data, but due to the heterogeneous distribution of such data the quality varies over the world. Nevertheless, with the advent of satellite gravity missions, it is today possible to recover the Moho constituents (i.e. Moho depth; MD and Moho density contrast; MDC) via gravity observations based on isostatic models. Prior to using gravity observations for this application it must be stripped due to the gravitational contributions of known anomalous crustal density structures, mainly density variations of oceans, glacial ice sheets and sediment basins (i.e. stripping gravity corrections). In addition, the gravity signals related mainly with masses below the crust must also be removed. The main purpose of this study is to estimate the significance of removing also remaining non-isostatic effects (RNIEs) on gravity, that is, gravity effects that remain after the stripping corrections. This is carried out by using CRUST19 seismic crustal model and employing Vening Meinesz–Moritz (VMM) gravimetric-isostatic model in recovering the Moho constituents on a global scale to a resolution of $1^\circ \times 1^\circ$. To reach this goal, we present a new model, named MHUU22, formed by the SGGUGM2 gravitational field, Earth2014 topography, CRUST1.0 and CRUST19 seismic crustal models. Particularly, this study has its main emphasis on the RNIEs on gravity and Moho constituents to find out if we can modify the stripping gravity corrections by a specific correction of the RNIEs. The numerical results illustrate that the RMS differences between MHUU22 MD and the seismic model CRUST1.0 and least-squares combined model MOHV21 are reduced by 33 and 41 per cent by applying the NIEs, and the RMS differences between MHUU22 MDC and the seismic model CRUST1.0 and least-squares combined model MDC21 are reduced by 41 and 23 per cent when the above strategy for removing the RNIEs is applied. Hence, our study demonstrates that the specific correction for the RNIEs on gravity disturbance is significant, resulting in remarkable improvements in MHUU22, which more clearly visualize several crustal structures.

Key words: Composition and structure of the continental crust; Composition and structure of the oceanic crust; Gravity anomalies and Earth structure; Moho depth; Remaining non-isostatic effect.

1 INTRODUCTION

Isostasy is a key concept in the Earth sciences describing the state of equilibrium (or mass balance) to which the mantle tends to balance the mass of the crust in the absence of external disturbing forces. One of most important application of the isostasy is to map the Moho discontinuity (or Moho), which separates the boundary between the Earth's crust and upper mantle. The Moho constituents (i.e. Moho depth or crustal depth; MD and Moho density contrast; MDC) are generally computed by two techniques of seismic and gravimetric. The seismic observations used in compiling global Moho models are typically sparse, and therefore interpolation of global MDs, particularly over areas without adequate seismic data, frequently yield unrealistic results with large uncertainties. Accordingly, over large parts of the world with a limited coverage of seismic data, the gravimetric or combination of seismic and gravimetric data is fruitfully offered (Abrehdary 2016). The gravimetric-isostatic approach uses the isostatic gravity anomaly (or disturbance) to model the Moho constituents. This anomaly/disturbance is the gravity signal

© The Author(s) 2023. Published by Oxford University Press on behalf of The Royal Astronomical Society. This is an Open Access article distributed under the terms of the Creative Commons Attribution License (https://creativecommons.org/licenses/by/4.0/), which permits unrestricted reuse, distribution, and reproduction in any medium, provided the original work is properly cited.

Downloaded from https://academic.oup.com/gji/article/234/3/2066/7152592 by Uppsala Universitetsbibliotek user on 16 June 2023

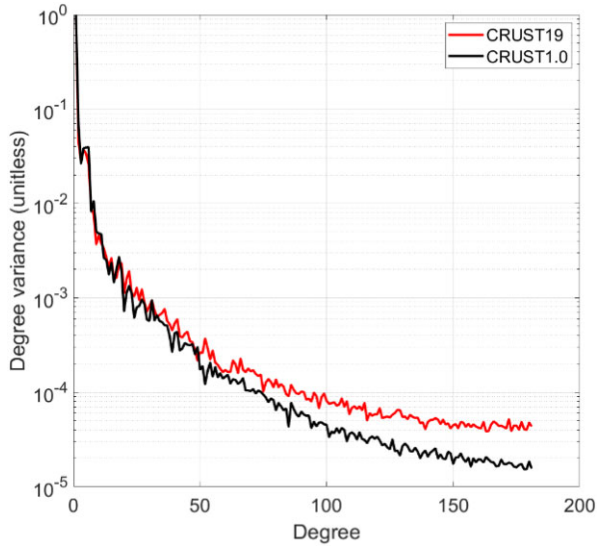

Figure 1. Degree variances of the CRUST1.0 and CRUST19 to degree 180.

corresponding to the isostatic compensation by the Moho constituents. Hence, the anomalous density structures not only within the crust but necessarily within the whole lithosphere (called the non-isostatic effects, NIEs) must be modelled and removed from the observed gravity signal, that is, the observed gravity data must be corrected in two main ways, namely for the gravitational contributions of mass density variations in different layers of the Earth's crust such as ice and sediment layers (stripping gravity corrections), as well as for the gravity contribution from deeper mass variations below the crust. Most of the NIEs are applied by removing lower degree harmonics of the gravity field (in this study harmonics at degrees $n < n_0 = 10$), which are assumed to be caused by deep Earth density variations, and by directly adding modelled stripping gravity corrections ('additive corrections') for ice, sediment, bathymetry, etc. (see below Section 2). However, one cannot expect to be able to remove all NIEs in this way. For instance, except for lacking stripping corrections there are also Moho constituents caused by techtonic motions in the Earth. Subsequently, the main purpose of this paper is to investigate if one can reach even better results by applying a technique to remove what we call remaining non-isostatic effects (RNIEs) on gravity. To do so, we will first recover the Moho constituents on global scale to a resolution of $1^\circ \times 1^\circ$ by employing the so-called Vening Meinesz-Moritz (VMM) technique (Sjöberg 2009; Sjöberg & Bagherbandi 2011), and we will then compare the outcomes with and without applying RNIEs using least-squares combined seismic and gravimetric-isostatic MD and MDC models (Sjöberg and Abrehdary 2022a, b) as well as the seismic model CRUST1.0 (Laske *et al.* 2013).

Up to now, several different isostatic models have been offered for mapping the MD and MDC before and after correcting for NIEs, and it is not specified which model is most suitable, which makes it difficult to judge what is the best method in a certain situation. Also, these studies usually used the same seismic model for determining the NIEs and also for the evaluation of their effects on the Moho constituents. For instance, the Bagherbandi & Sjöberg (2012) calculated NIEs on crustal thickness using CRUST2.0 in Fennoscandia and they concluded that the final result for the Moho could be considered as bias-free. See also Bagherbandi *et al.* (2013).

Unlike previous studies, we now include additional information such as stripping gravity corrections as well as using the seismic crustal model CRUST19 (Szwillus *et al.* 2019) in estimating the RNIEs, leading to a new Moho model named MHUU22 containing both MD and MDC by using data sets of the SGGUGM2 gravitational field (Liang *et al.* 2020), Earth2014 topography (Hirt & Rexer 2015), CRUST1.0 and CRUST19 seismic crustal models. This model will be evaluated by comparing it with CRUST1.0, MOHV21 and MDC21 models (Sjöberg and Abrehdary 2022a, b). The MHUU22 model includes uncertainty estimates. (It is worth noting that error estimates of MD and MDC are of great importance to any usage of Moho models. Nevertheless, the evaluation of such uncertainties are usually overlooked.)

2 MOHO RECOVERY

2.1 The concept of the VMM method

The VMM inverse problem of isostasy aims at estimating the MD in such way that the isostatic compensating attraction $A_C(P)$ of the crustal mass totally compensates the Bouguer gravity disturbance on the Earth's surface, $\delta g_B^{\mathrm{TBISN}}$, which is corrected for the gravitational contributions of topography/bathymetry and density contrasts of the oceans, ice and sediments and also RNIEs. Assuming that the MDC ($\Delta\rho$) is known, Sjöberg (2009) showed that this constraint leads to a nonlinear Fredholm integral equation in MD (denoted D below), whose second-order solution becomes:

$$D(P) = D_1(P) + \frac{D_1^2(P)}{R} - \frac{1}{32\pi R}\iint_{\sigma} \frac{D_1^2(Q) - D_1^2(P)}{\sin^3(\psi/2)} d\sigma_Q \tag{1}$$

where R is sea level radius, σ is the unit sphere. D_1 is a first-order approximation, defined by the spectral form:

$$D_1(P) = \sum_{n=n_0}^{\infty}\left(2 - \frac{1}{n+1}\right)\sum_{m=-n}^{n} f_{nm} Y_{nm}(P), \tag{2}$$

where f_{nm} is the negative spherical harmonic coefficient of $\delta g_B^{\mathrm{TBISN}}$ divided by the gravitational constant times density contrast and Y_{nm} is the fully normalized spherical harmonic of degree n and order m. n_0 is set to 10 under the assumption that the lower degrees are all created by gravity disturbances in the deep mantel and Earth's core.

Sjöberg & Bagherbandi (2011) showed that the above Fredholm equation could also yield similar solutions to the MDC for known MD and to the product of MD and MDC. See also Sjöberg & Bagherbandi (2017, p. 306).

3 ADDITIVE CORRECTIONS TO THE GRAVITY DISTURBANCE

As already presented in the Introduction, gravity data contain signals of the whole spectrum of the Earth's structure, that is, signals from the geometries and density distributions of topography and bathymetry, ice and sediment layers as well as variable density layers in the mantle and core/mantle topographic variations. Here we assume that the long-wavelength contribution to the gravity field, say to degree and order 10, is related to the mantle as well as core–mantle boundary topography (Sjöberg 2009). To strip the gravity data caused only by the geometry and density contrast of the Moho interface, all aforementioned signals contributors to the gravity data should be removed by applying the so-called stripping gravity corrections as well as RNIEs.

Downloaded from https://academic.oup.com/gji/article/234/3/2066/7152592 by Uppsala Universitetsbibliotek user on 16 June 2023

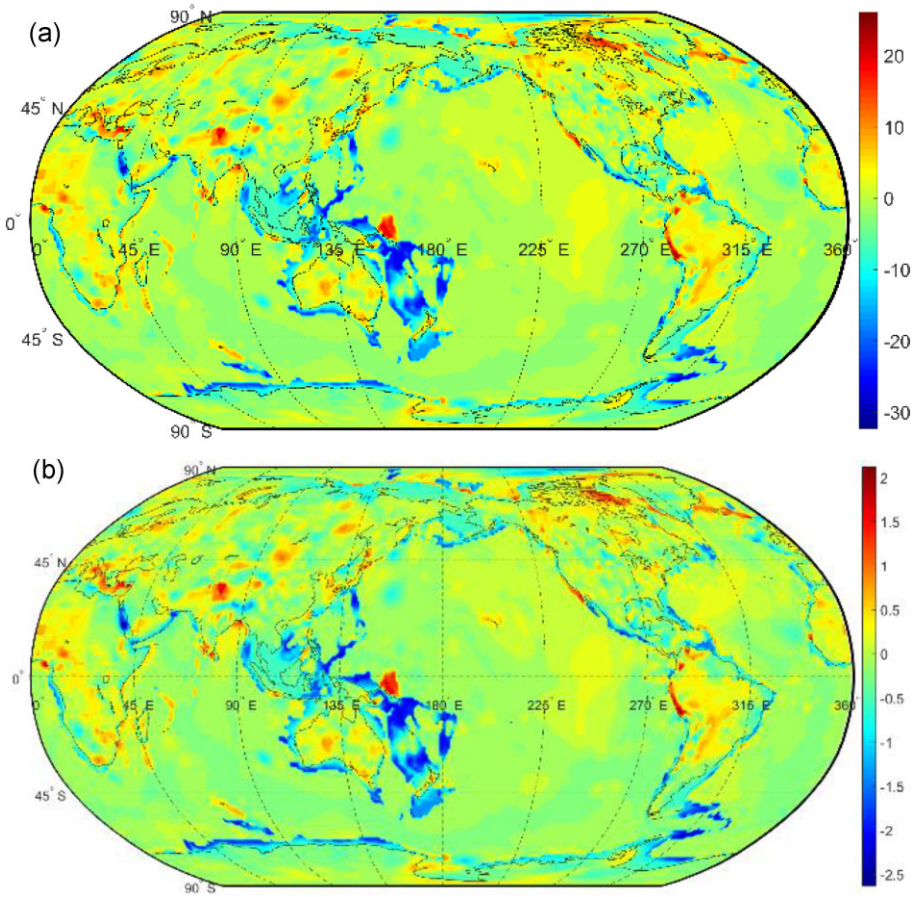

Figure 2. (a) The MD differences CRUST1.0 minus CRUST19, and (b) the corresponding standard error differences.

3.1 Stripping gravity corrections

The main input data set used in the VMM method is the the refined Bouguer gravity disturbances, δg_B^{R1}, that is, free-air gravity disturbances corrected for topography, bathymetry, ice thickness and sediment basins (stripping gravity corrections δg^{TBIS}; see Tenzer *et al.* 2015).

The refined Bouguer gravity disturbance δg_B^{R1} is thus realized from the SGGUGM2 free-air gravity disturbance $\delta g_{\mathrm{FA}}^{\mathrm{SGGUGM2}}$ by:

$$\delta g_B^{R1} = \delta g_{\mathrm{FA}}^{\mathrm{SGGUGM2}} - \delta g^{\mathrm{TBIS}}. \quad (3)$$

3.2 Remaining NIEs

It needs to be mentioned to the reader that in general the crust is not in complete isostatic equilibrium, and the observed gravity data are not only generated by the topographic/isostatic masses, but also from masses in the deep Earth interior, that lead to the NIEs. Typically, the NIEs are divided into two groups. The first group comprises those effects that, if they were corrected for, make the isostatic gravity anomaly/disturbance consistent with the Moho in isostatic balance. In reality, the Moho is not only formed by isostasy, but there are other causes, which affect the crustal thickness estimation. Hence, in contrast to above, the second group are those gravitational effects that are caused by the deviation of the Moho from its isostatic model.

According to Sjöberg (2009) the major part of the long wavelengths of the geopotential are caused by density variations in the Earth's mantle and core/mantle topography variations. Such NIEs could be the contribution of different factors, such as crustal thickening/thinning, thermal expansion of mass of the mantle (Kaban *et al.* 2004), Glacial Isostatic Adjustment (GIA), plate flexure (Watts 2001, p. 114) and effect of other phenomena (Tenzer *et al.* 2009). This implies that this contribution to gravity will lead to systematic errors/NIEs of the computed Moho topography and density contrast. Hence, the NIEs should also be corrected on the isostatic gravity disturbance.

It needs a trustworthy seismic Moho model for its implementation. It is worth mentioning that, there are already some global crust models based on seismic methods. CRUST1.0 is the most frequently used crustal model, which is based on a database of crustal thickness data from active source seismic studies as well as from receiver function studies. More recently, Szwillus *et al.* (2019) developed a global crustal thickness model and velocity structure from geostatistical analysis of seismic data (i.e. CRUST19). In this section, a short discussion on which seismic model should be used for best estimating the RNIEs is presented among the two selected candidate models CRUST1.0 and CRUST19. To do so, we first compare their power spectra to degree 180 in Fig. 1, showing that the spectra are close in the low degrees (say, to degrees 10), but then the power of CRUST19 decreases significantly slower than that for CRUST1.0.

In Fig. 2(a), we plot the difference between CRUST1.0 and CRUST19, whereas in Fig. 2(b), the difference between two models divided by the standard deviation of CRUST19 is plotted, showing that the largest differences occur in South America and Asia, otherwise the two models are overall similar. However, disagreements are observed in the continent-ocean transition which could

Downloaded from https://academic.oup.com/gji/article/234/3/2066/7152592 by Uppsala Universitetsbibliotek user on 16 June 2023

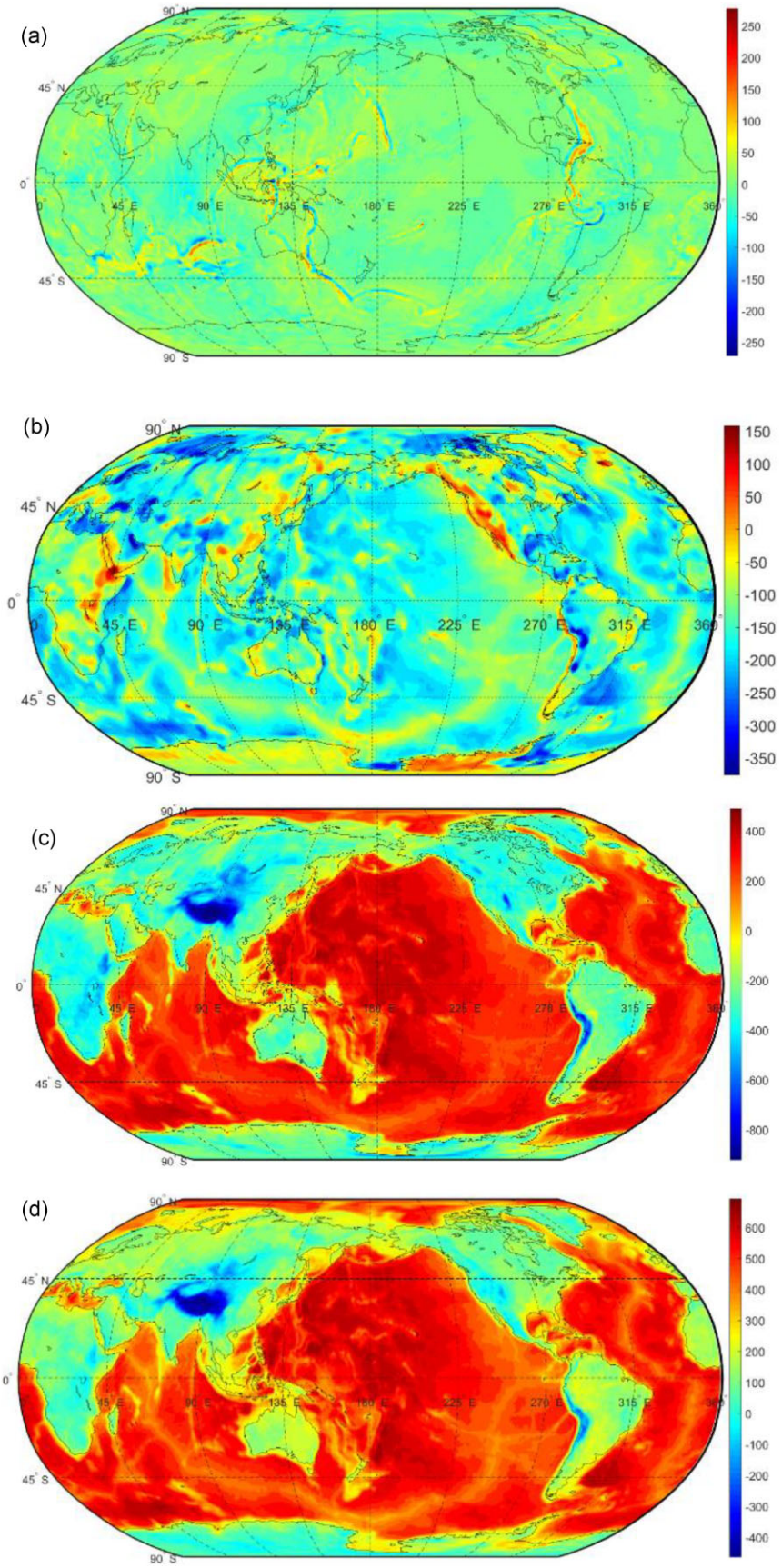

Figure 3. (a) The free-air gravity disturbances produced by the SGGUGM2, (b) the RNIEs, (c) the refined Bouguer gravity disturbances not corrected for RNIEs and (d) the refined Bouguer gravity disturbances corrected for RNIEs (unit: mGal).

Downloaded from https://academic.oup.com/gji/article/234/3/2066/7152592 by Uppsala Universitetsbibliotek user on 16 June 2023

Table 1. Statistics of the free-air and refined Bouguer gravity disturbance estimated from SGGUGM2 model. STD is the standard deviation of the estimated quantities over the study area, $\delta g_{\mathrm{FA}}^{\mathrm{SGGUGM2}}$ is free-air gravity disturbance, δg^{TBIS} is Bouguer gravity disturbance corrected for topography, bathymetry, ice thickness and sediment basins (i.e. stripping gravity corrections), $\delta g^{\mathrm{RNIEs}}$ is gravity disturbance corrected for RNIEs and $\delta g_R^{\mathrm{TBISN}}$ is gravity disturbance corrected for stripping gravity corrections as well as RNIEs.

Unit	Quantities	Max.	Mean	Min.	STD
mGal	$\delta g_{\mathrm{FA}}^{\mathrm{SGGUGM2}}$	287.53	− 0.44	− 281.06	23.86
	δg^{TBIS}	514.40	36.40	− 945.99	276.80
	$\delta g^{\mathrm{RNIEs}}$	167.25	− 134.65	− 385.12	62.23
	$\delta g_R^{\mathrm{TBISN}}$	655.59	329.40	− 474.92	200.51

Table 2. Statistics of the MD and MDC estimated from MHUU22 model. STD is the standard deviation of the estimated quantities over the study area, PMHUU22 MD is the (preliminary) MD, estimated from MHUU22 model, before applying the stripping gravity corrections and RNIEs effect, MHUU22 MD is the final MD estimated from MHUU22 model, after applying the stripping gravity corrections and RNIEs. And, PMHUU22 MDC is the (preliminary) MDC, estimated from MHUU22 model, before applying the stripping gravity corrections and RNIEs effect, MHUU22 MDC is the final MDC estimated from MHUU22 model, after applying the stripping gravity corrections and RNIEs. STD-MHUU22 MD and STD-MHUU22 MDC are the standard errors of the MHUU22 MD/MDC after applying RNIE corrections.

Unit	Quantities	Max.	Mean	Min.	STD
km	PMHUU22 MD	56.51	22.05	8.53	11.07
	MHUU22 MD	67.58	23.19	8.53	12.55
	STD-MHUU22 MD	6.89	0.82	0.14	0.54
$\mathrm{kg\,m^{-3}}$	PMHUU22 MDC	636.66	322.13	21.06	105.85
	MHUU22 MDC	751.42	339.96	69.42	129.96
	STD-MHUU22 MDC	81.09	20.14	1.06	14.29

be explained by the fact that CRUST1.0 uses a smooth transition over the continental margin, while CRUST19 uses a sharp jump from continental to oceanic crust leading to a systematic difference between CRUST19 and CRUST1.0 on the edges of the continents (see Szwillus *et al.* 2019). The assessment of the global Moho models of CRUST1.0 and CRUST19 is not an easy task, but the RMS differences between the two are typically of the order of 4.5 km and reduces to 3.3 km when exempting S. America.

Next, we will rely on CRUST19 model for estimating the RNIEs, as CRUST19 is based on a USGS database of crustal seismic studies including little additional information, following a design philosophy that tries to respect the data as much as possible. This model interpolates MD and average - wave velocity of the crystalline crust using a non-stationary kriging algorithm. A major advantage is that the model is relatively straightforward in deriving the uncertainties.

If we assume that CRUST19 is known and correct, the gravity effect of the RNIEs can be estimated from its difference to the observed gravity effect:

$$\delta g^{\mathrm{RNIEs}} = \frac{GM}{R^2}\sum_{n=0}^{n_{\max}}(n+1)\sum_{m=-n}^{n} c_{nm}^{\mathrm{RNIEs}} Y_{nm}\,(\mathrm{P}), \tag{4a}$$

where

$$c_{nm}^{\mathrm{RNIEs}} = c_{nm}^{\mathrm{CRUST19}} - c_{nm}^{\mathrm{VMM}}. \tag{4b}$$

Here, c_{nm}^{RNIEs}, c_{nm}^{VMM} and $c_{nm}^{\mathrm{CRUST19}}$ are the spherical harmonic coefficients of the gravity disturbances of the RNIEs, VMM and CRUST19, respectively.

The spherical harmonic coefficients c_{nm}^{j} (j = VMM, CRUST19) in eq. (4b) are generated using the following expression (see Bagherbandi *et al.* 2017):

$$c_{nm}^{j} \approx \frac{3}{(2n+1)\,R\rho_e}\left[\left(\Delta\rho\,(D_j - D_0)\right)_{nm} + \frac{(n+2)\left(\Delta\rho(D_0^2 - D_j^2)\right)_{nm}}{2R^2}\right] \tag{4c}$$

Here $\rho_e(\approx 5.5\ \mathrm{g\,cm^{-3}})$ is the Earth's mean density, $R(= 6371 \times 10^3\ \mathrm{m})$ is the Earth's mean radius (which approximates the geocentric radius of the geoid surface), D_{VMM}, D_{CRUST19} and D_0 are the MDs of VMM, CRUST19 and their global mean value (approximately 23 km based on CRUST19 model), respectively. $\Delta\rho$ is the (assumed) constant MDC and the spherical harmonic coefficients $(\Delta\rho(D_j - D_0))_{nm}$, $(\Delta\rho(D_j^2 - D_0^2))_{nm}$ are defined for the following products of the MDC and MD: $\Delta\rho(D_j - D_0)$, $\Delta\rho(D_j^2 - D_0^2)$.

Taking into consideration the gravitational contribution of the crust density heterogeneous, the NIEs are applied to the isostasy gravity disturbance δg_I. The refined Bouguer gravity disturbance in eq. (3) is then rewritten as:

$$\delta g_B^{R2} = \delta g_B^{R1} - \delta g^{\mathrm{RNIEs}}. \tag{5}$$

4 DATA

As we already mentioned, the main goals of this investigation are to compute RNIEs on gravity by using the CRUST19 seismic crustal model and to use the VMM model in imaging the Moho constituents on a global scale to a resolution of $1^\circ \times 1^\circ$. To that end, we deliver a new model, named MHUU22, including MD and MDC estimated from the SGGUGM2 gravitational field, Earth2014 topography, CRUST1.0 and CRUST19 seismic crustal models. SGGUGM2 is a new high-resolution Earth gravity field model from satellite gravimetry, satellite altimetry and Earth Gravitational Model 2008 (EGM2008)-derived gravity data based on the theory of the ellipsoidal harmonic analysis and coefficient transformation (Liang *et al.* 2020).

The refined Bouguer gravity disturbances were generated using the SGGUGM2 Earth gravitational model coefficients and DTM2006 topographic model (Pavlis *et al.* 2007), complete to degree and order 180 of spherical harmonics, and the spherical harmonics of the normal gravitational field were computed according to the parameters of the reference system GRS-80 (Moritz 2000). Then these gravity disturbances were corrected for the density variation of the oceans, ice sheets and sediment basins (i.e. δg_B^{R1}; see Tenzer *et al.* 2015) and also the RNIEs (Bagherbandi & Sjöberg 2013), (see eqs 3 and 5). As already stated, we follow the method presented by Bagherbandi & Sjöberg (2012) to estimate RNIEs on gravity using the recent seismic crustal thickness in CRUST19 model by comparing the gravimetric and seismic data in the frequency domain. CRUST19 is also used to obtain the nominal MD (D_0).

Figs 3(a) and (b) plot the free-air gravity disturbances computed by SGGUGM2 and the RNIEs estimated by CRUST19, whereas Figs 3(c) and (d) depict the refined Bouguer gravity disturbances stripped by the bathymetry, ice, sediment variations before and after applying the RNIEs. Comparing Figs 3(a) and (c) show considerable modifications over oceans due to the bathymetric stripping gravity corrections, and also in central Greenland and Antarctica due to the correction for ice density variation and also for sediment stripping over sediment basins. However, a comparison of Figs 3(c) and (d)

Downloaded from https://academic.oup.com/gji/article/234/3/2066/7152592 by Uppsala Universitetsbibliotek user on 16 June 2023

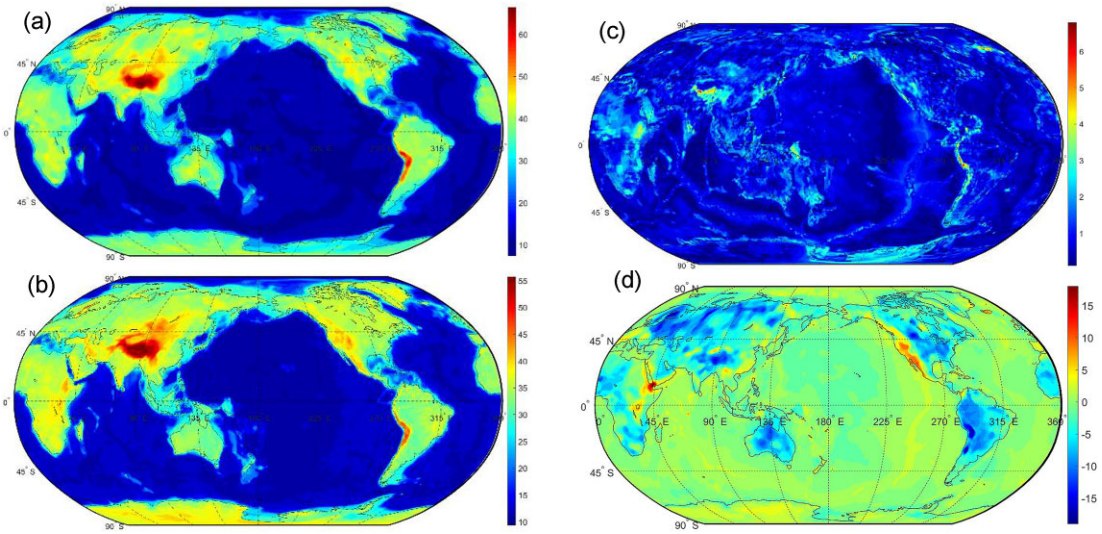

Figure 4. The estimated MD (a) corrected for RNIEs, (b) not corrected for RNIEs. (c) The standard error of the MHUU22 MD after applying RNIE corrections (unit: km).

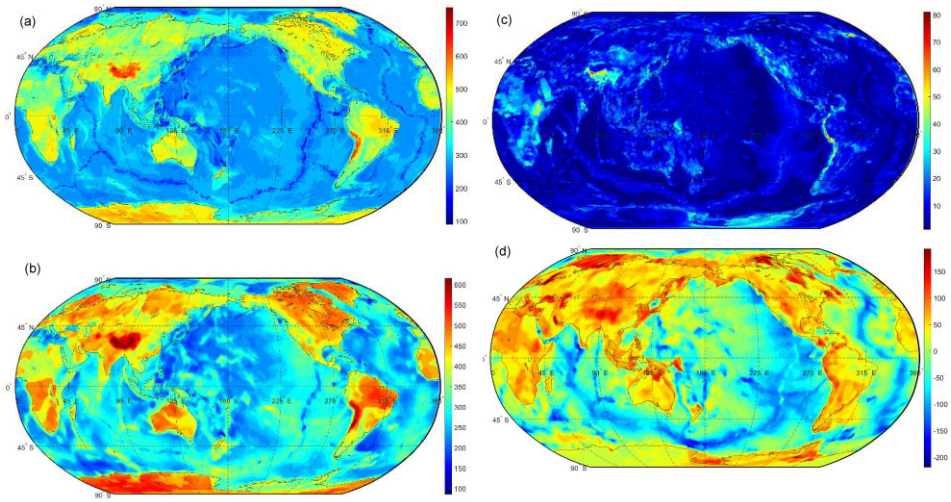

Figure 5. The estimated MDC (a) corrected for RNIEs, (b) not corrected for RNIEs. (c) The standard error of the MHUU22 MDC after applying RNIE corrections (unit: kg m^{-3}).

Table 3. Comparisons of MHUU22 with CRUST1.0, MOHV21 and MDC21 models. STD is the standard deviation of the estimated quantities over the study area. RMS is the roote mean square error. PMHUU22 models are preliminary models not corrected for NIEs.

Unit	Differences	Max.	Mean	Min.	STD	RMS
km	PMHUU22 MD – CRUST1.0	15.45	– 2.66	– 21.64	3.89	4.6
	PMHUU22 MD – MOHV21	11.35	– 1.10	– 20.26	2.45	2.7
	MHUU22 MD – CRUST1.0	13.39	– 0.96	– 14.69	3.12	3.16
	MHUU22 MD – MOHV21	6.49	0.98	– 4.45	1.00	1.6
kg m^{-3}	PMHUU22 MDC – CRUST1.0	360.21	– 9.12	– 485.84	112.68	109.3
	PMHUU22 MDC – MDC21	200.25	9.65	– 187.14	67.97	67.2
	MHUU22 MDC – CRUST1.0	241.65	– 10.14	– 348.79	64.97	64.2
	MHUU22 MDC – MDC21	289.79	9.14	– 141.135	51.55	51.6

Downloaded from https://academic.oup.com/gji/article/234/3/2066/7152592 by Uppsala Universitetsbibliotek user on 16 June 2023

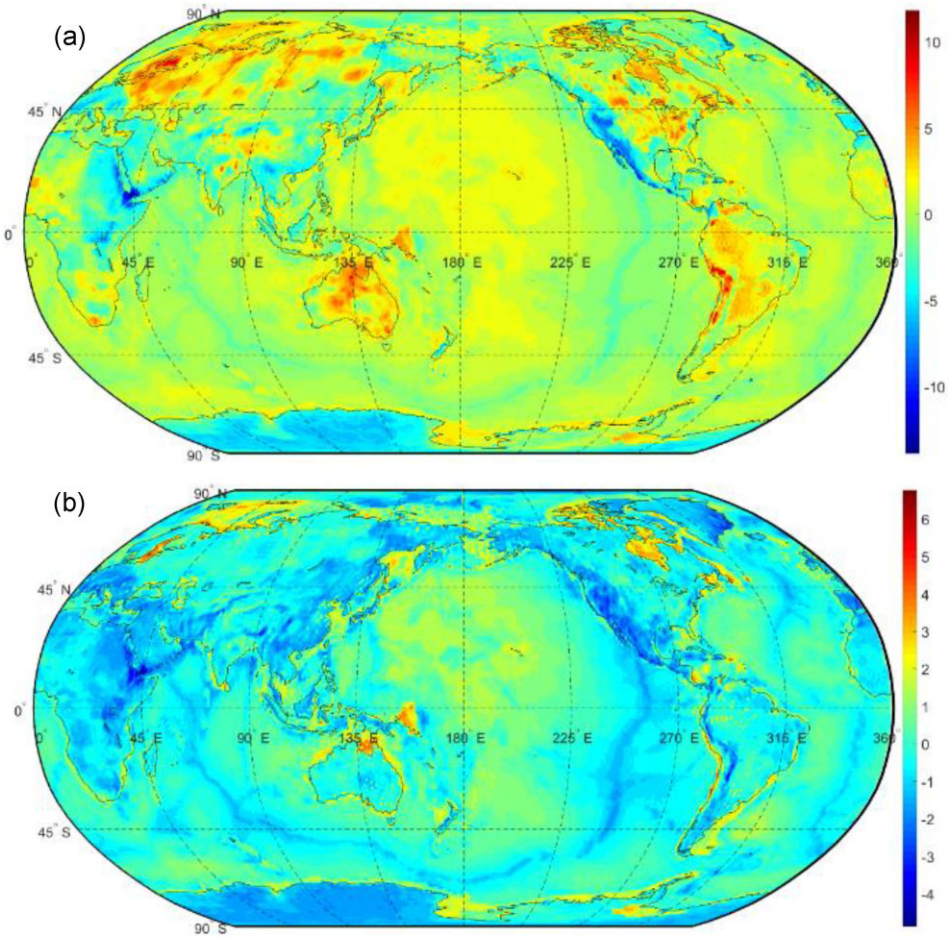

Figure 6. (a) The MD differences between the MHUU22 and CRUST1.0 and (b) the differences between the MHUU22 and MOHV21 (unit: km).

clearly shows significant effects of applying the RNIEs, most obvious along the mid ocean ridges (see also Sjöberg & Abrehdary 2021a). In the open seas, the RNIEs could also be determined based on empirical formulas related with the inverse crustal ageing (e.g. Seton *et al.* 2020) and/or the lithospheric thermal-pressure variations (e.g. Bagherbandi *et al.* 2017).

We finally calculate the correlation coefficients for the oceanic lithosphere age (Müller *et al.* 2008) versus RNIE, MD and MDC are −0.56, −0.49 and −0.35, respectively.

5 RESULTS

5.1 MD and MDC estimation along with their uncertainties

In this section, we employ the VMM model to estimate the Moho constituents (i.e. MD and MDC) on global scale in a set of $1^\circ \times 1^\circ$ blocks. In this way, different heterogeneous data are used, including the global Earth gravity field model (e.g. SGGUGM2), the global topography model (e.g. Earth2014) and the global seismic crustal model (e.g. CRUST1.0 and CRUST19). In the following, we map the free-air gravity disturbances produced by the SGGUGM2 model, RNIEs deducted by CRUST19, and the refined Bouguer gravity disturbances after applying RNIE corrections **(**see Table 1**).**

In order to calculate the standard errors of the MHUU22 MD/MDC, we follow the strategy explained by Sjöberg & Abrehdary (2021b) based on an optimal least-squares combination of seismic and gravimetric-isostatic models of MD or MDC at a resolution of $1^\circ \times 1^\circ$.

Finally, the MHUU22 MD and MDC models are geophysically interpreted along with their standard errors in Table 2 and Figs 4 and 5(c).

Figs 4(a) and (b) plot the MD estimated from the MHUU22 model after and before applying the correction for the RNIEs, and similar comparison for MDC are shown in Figs 5(a) and (b). As one would already expect, in most areas there are remarkable changes. For example, the shallow MDs with large MDCs along mid-ocean ridges become more pronounced, and significantly deeper MDs with larger MDCs are also seen in the Himalayas and the S. American west coast. Similar effects can also be seen in areas with post-glacial rebound (e.g. Fennoscandia and Hudson Bay in Canada). In areas with existing huge ice masses (Antarctica and Greenland) the MD is also significantly modified.

Figs 4(c) and 5(c) map the MHUU22 MD and MDC standard errors, showing errors smaller than 3 km and 30 kg m^{-3} in oceanic regions, while for continental regions the errors reach 6 km and 70 kg m^{-3}.

Downloaded from https://academic.oup.com/gji/article/234/3/2066/7152592 by Uppsala Universitetsbibliotek user on 16 June 2023

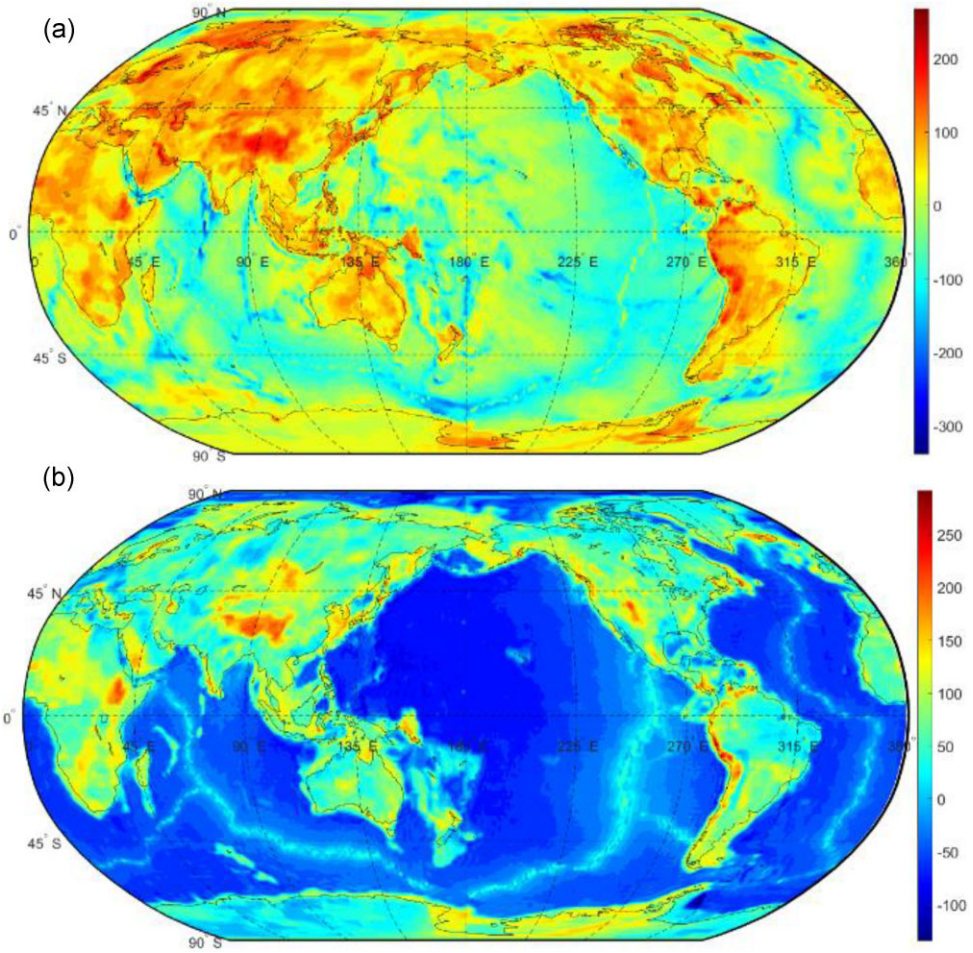

Figure 7. (a) The MDC differences between the MHUU22 and CRUST1.0 and (b) the differences between the MHUU22 MDC and MDC21 (unit: kg m^{-3}).

5.2 Assessment of MHUU22 MD/MDC

The main aim of this section is to assess the quality of MHUU22 MD/MDC with respect to some other global models. To do so, we compare MHUU22 before/after correcting for RNIEs (PMHU22/MHUU22) with CRUST1.0, MOHV21 and MDC21.

MOHV21 (Sjöberg & Abrehdary 2022a) is a-n MD model based on an optimal least-squares combination of five global seismic and gravimetric-isostatic models at a resolution of 1° × 1°, while MDC21 (Sjöberg & Abrehdary 2022b) is a new global MDC model based on a weighted least-squares combination of three available MDC models at a resolution of 1° × 1°. Table 3 demonstrates significant improved agreements in the comparisons when applying the NIEs, in particular in the RMS. In the comparisons with MOHV21 and MDC21, there are reductions of 40 and 23 per cent, respectively.

In the upper part of Table 3 (also in Figs 6a and b), the MDs estimated by MHUU22 are compared with those in CRUST1.0 and MOHV21, respectively, showing that the RMS differences between MHUU22 and CRUST1.0 and MOHV21 are 3.1/4.6 and 1.6/2.7 km before/after considering the RINE corrections. In the lower part of Table 3 (along with Figs 7a and b), we compare the MDC of MHUU22 with CRUST1.0 and MDC21. In summary, the RMS difference between MHUU22 MDC and CRUST1.0 is 64.2/109.3 kg m^{-3} and the comparison with MDC21 yields 51.6/67.2 kg m^{-3} before/after applying the RINE corrections, respectively.

7. CONCLUSIONS

The main focus of this paper was to estimate the RNIEs on gravity using a seismic Moho model (CRUST19). For this purpose, the refined Bouguer gravity disturbance was primarily reduced for gravity of topography, density heterogeneities related to bathymetry, ice, sediments and other crustal components using stripping gravity corrections, and it was further corrected for RNIEs of nuisance gravity signals from mass anomalies below the crust due to crustal thickening/thinning, thermal expansion of the mantle, Delayed Glacial Isostatic Adjustment (DGIA) and plate flexure. We then delivered a new gravimetric-isostatic MHUU22 model including the MD and MDC using the VMM gravimetric-isostatic model from the refined Bouguer gravity disturbance and Earth2014 topographic data.

We also validated the RMS of differences between MHUU22 MD and the seismic model CRUST1.0 and MOHV21 when applying the RNIE corrections, yielding reductions of 33 and 41 per cent, respectively. Similarly, the RMS difference of MHUU22 MDC and the seismic model CRUST1.0 and MOHV21 reduced 41 and 23 per cent, respectively. Hence, the specific corrections for the RNIEs on gravity disturbance is significant, resulting in expected noteworthy changes in MHUU22 towards the optimal least-squares models. For instance, this implies that only the RNIE corrected Figs 4(a) and 5(a) clearly show small MDs and MDCs that are typical along the mid ocean ridges. Also the regional MD maxima in NW China (about 59 km) and central Finland (about 57 km) are only visible after correcting for the RNIE (Fig. 4a).

Downloaded from https://academic.oup.com/gji/article/234/3/2066/7152592 by Uppsala Universitetsbibliotek user on 16 June 2023

ACKNOWLEDGMENTS

This study was supported by project no. 187/18 of the Swedish National Space Agency (SNSA).

DATA AVAILABILITY

The data sets generated and/or analysed during this study are available from the first author on reasonable request.

REFERENCES

Abrehdary, M., 2016. *Recovering Moho Parameters Using Gravimetric and Seismic Data (Doctoral Dissertation,* KTH Royal Institute of Technology.

Bagherbandi, M., Bai, Y., Sjöberg, L.E., Tenzer, R., Abrehdary, M., Miranda, S. & Sanchez, J.M.A., 2017. Effect of the lithospheric thermal state on the Moho interface: a case study in South America. *J. South Amer. Earth Sci.,* **76,** 198–207.

Bagherbandi, M. & Sjöberg, L.E., 2012. Non-isostatic effects on crustal thickness:a study using CRUST2.0 in Fennoscandia. *Phys. Earth planet. Inter.,* **200-201,** 37–44

Bagherbandi, M. & Sjöberg, L.E., 2013. Improving gravimetric–isostatic models of crustal depth by correcting for non-isostatic effects and using CRUST2. 0. *Earth Sci. Rev.,* **117,** 29–39.

Bagherbandi, M., Tenzer, R., Sjöberg, L.E. & Novák, P., 2013. Improved global crustal thickness modeling based on the VMM isostatic model and non-isostatic gravity correction. *Journal of Geodynamics,* **66,** 25–37.

Hirt, C. & Rexer, M. 2015., Earth2014: 1 arc-min shape, topography, bedrock and ice-sheet models–Available as gridded data and degree-10,800 spherical harmonics. *Int. J. Appl. Earth Obs. Geoinf.,* **39,** 103–112.

Kaban, M. K., Schwintzer, P. & Reigber, C., 2004. A new isostatic model of the lithosphere and gravity field. *J. Geod.,* **78**(6), 368–385.

Laske, G., Masters, G., Ma, Z. & Pasyanos, M., 2013, April, Update on CRUST1.0—a 1-degree global model of Earth's crust, in *Geophys. Res. Abstr*(Vol., **15,** p. 2658). Vienna, Austria: EGU General Assembly.

Liang, W., Li, J., Xu, X., Zhang, S. & Zhao, Y., 2020. A high-resolution Earth's gravity field model SGG-UGM-2 from GOCE, GRACE, satellite altimetry, and EGM2008. *Engineering,* **6**(8), 860–878.

Moritz, H., 2000. Geodetic reference system 1980. *J. Geod.,* **74**(1), 128–133.

Müller, R.D., Sdrolias, M., Gaina, C. & Roest, W.R., 2008. Age, spreading rates, and spreading asymmetry of the world's ocean crust. *Geochem. Geophys. Geosyst.,* **9**(4). doi:10.1029/2007GC001743.

Pavlis, N.K., Factor, J.K. & Holmes, S.A., 2007. Terrain-related gravimetric quantities computed for the next EGM, in *Proceedings of the 1st International Symposium of the International Gravity Field Service (IGFS)*. Istanbul, 318–323.

Seton, M., *et al.*, 2020. A global data set of present-day oceanic crustal age and seafloor spreading parameters. *Geochem. Geophys. Geosyst.,* **21**(10), e2020GC009214. doi:10.1029/2020GC009214.

Sjöberg, L.E., 2009. Solving Vening Meinesz-Moritz inverse problem in isostasy. *Geophys. J. Int.,* **179**(3), 1527–1536.

Sjöberg, L.E. & Abrehdary, M., 2021a. On Moho determination by the Vening Meinesz-Moritz technique, in *Geodetic Sciences-Theory, Applications and Recent Developments*. IntechOpen.

Sjöberg, L.E. & Abrehdary, M., 2021b. The uncertainty of CRUST1.0. *J. appl. Geod.,* **15**(2), 143–152.

Sjöberg, L.E. & Abrehdary, M., 2022a. MOHV21: a least squares combination of five global Moho depth models. *J. Geod.,* **96**(6), 1–8.

Sjöberg, L.E. & Abrehdary, M., 2022b. Combination of three global Moho density contrast models by a weighted least-squares procedure. *J. appl. Geod*., **16**(4), pp. 331–339.

Sjöberg, L.E. & Bagherbandi, M., 2011. A method of Estimating the Moho density contrast with a tentative application of EGM08 and CRUST2.0. *Acta Geophys.* **59**(3), 502–525.

Sjöberg, L.E. & Bagherbandi, M., 2017. *Gravity Inversion and Integration*. Basel, Switzerland: Springer International Publishing AG.

Szwillus, W., Afonso, J.C., Ebbing, J. & Mooney, W.D., 2019. Global crustal thickness and velocity structure from geostatistical analysis of seismic data. *J. geophys. Res.: Solid Earth,* **124**(2), 1626–1652.

Tenzer, R., Chen, W., Tsoulis, D., Bagherbandi, M., Sjöberg, L.E., Novák, P. & Jin, S., 2015. Analysis of the refined CRUST1. 0 crustal model and its gravity field. *Surv. Geophys.,* **36**(1), 139–165.

Tenzer, R., Hamayun, K. & Vajda, P., 2009. Global maps of the CRUST 2.0 crustal components stripped gravity disturbances. *J. geophys. Res.: Solid Earth,* **114**(B5). doi:10.1029/2008JB006016.

Watts, A.B., 2001. *Isostasy and Flexure of the Lithosphere*. Cambridge University Press.

Downloaded from https://academic.oup.com/gji/article/234/3/2066/7152592 by Uppsala Universitetsbibliotek user on 16 June 2023

© The Author(s) 2023. Published by Oxford University Press on behalf of The Royal Astronomical Society. This is an Open Access article distributed under the terms of the Creative Commons Attribution License (https://creativecommons.org/licenses/by/4.0/), which permits unrestricted reuse, distribution, and reproduction in any medium, provided the original work is properly cited.